Published in final edited form as:
Proteomics. 2009 November ; 9(21): 4920–4933. doi:10.1002/pmic.200800836.

Proteome changes in human broncho-alveolar cells following styrene exposure indicate involvement of oxidative stress in the molecular response mechanism

Nora Mörbt[1], **Iljana Mögel**[2], **Stefan Kalkhof**[1], **Ralph Feltens**[1,2], **Carmen Röder-Stolinski**[2], **Jiang Zheng**[3], **Carsten Vogt**[4], **Irina Lehmann**[2], and **Martin von Bergen**[1,5]

[1]Department of Proteomics, UFZ, Helmholtz-Centre for Environmental Research, Permoserstr. 15, 04318 Leipzig, Germany

[2]Department of Environmental Immunology, UFZ, Helmholtz-Centre for Environmental Research, Permoserstr. 15, 04318 Leipzig, Germany

[3]Center for Developmental Therapeutics, Seattle Children's Hospital Research Institute, Division of Gastroenterology, Department of Pediatrics, School of Medicine, University of Washington, Seattle, WA 98101, USA

[4]Department of Isotope Biogeochemistry, UFZ, Helmholtz-Centre for Environmental Research, Permoserstr. 15, 04318 Leipzig, Germany

[5]Department of Metabolomics, UFZ, Helmholtz-Centre for Environmental Research, Permoserstr. 15, 04318 Leipzig, Germany

Abstract

Styrene is a volatile organic compound (VOC) that is widely used as an intermediate in many industrial settings. There are known adverse health effects at environmentally significant concentrations, but little is known about the molecular effect of exposure to styrene at subacute toxic concentrations. We exposed human lung epithelial cells, at a wide range of concentrations (1 mg/m^3-10 g/m^3), to styrene and analyzed the effects on the proteome level by 2-DE, where 1,380 proteins spots were detected and 266 were identified unambiguously by mass spectrometry. A set of 16 protein spots was found to be significantly altered due to exposure to styrene at environmentally significant concentrations of 1-10 mg/m^3 (0.2 – 2.3 ppm). Among these, superoxide dismutase [Cu-Zn] as well as biliverdin reductase A could be correlated with the molecular pathway of oxidative stress, while eukaryotic translation initiation factor 5A-1, ezrin, lamin B2 and voltage dependent anion channel 2 have been reported to be involved in apoptosis. Treatment with styrene also caused formation of styrene oxide-protein adducts, specifically for thioredoxin reductase 1. These results underline the relevance of oxidative stress as a primary molecular response mechanism of lung epithelial cells to styrene exposure at indoor-relevant concentrations.

Keywords

Indoor air; Oxidative stress; Styrene; Styrene oxide-protein adducts; VOC

Correspondence: PD Dr. Martin von Bergen, UFZ, Helmholtz-Centre for Environmental Research, Department of Proteomics, Permoserstr. 15, 04318 Leipzig, Germany Martin.vonbergen@ufz.de**Fax:** +49-341-2351786.

1 Introduction

Changes in life-style, accompanied by prolonged times spent indoors and the widespread usage of volatile organic compounds (VOCs) in consumer products, have led to an extensive exposure to these chemicals, contributing to the aetiology of the sick building syndrome (see [1, 2] for review).

VOCs can be divided into two common classes, the aromatic and the aliphatic hydrocarbons, among which especially the halogenated aromatic compounds occur in high abundance, with many structural variations [3]. Among the non-halogenated substances, styrene, of which 14 million tons were produced in the European Union in 1992 [4], is one of the most important contaminants released from indoor sources. This aromatic VOC is widely used in consumer products, such as solvents, paints, glues, packing and insulation materials, pipes and carpet backing. Due to its low vapour pressure, styrene is highly volatile and therefore one of the most important chemicals in indoor environments [3, 5].

Although inhalation is the most important route of styrene exposure [6], metabolic conversion has been reported to take place predominantly in the liver. Styrene is mainly metabolized by cytochrome P450 monoxygenases to styrene oxide (SO). This reaction leads to S- and R-forms of SO, which exerts its toxicity possibly via DNA adduct formation. SO-modified proteins, such as albumin and hemoglobin, have been detected in animals and humans after exposure to styrene [7, 8]. Apart from that, little is known about the interaction of SO with cellular proteins [9, 10]. For lower levels of styrene exposure, such as concentrations of below 1 mg/m^3, no acute toxic effects have been described so far. However, induction of inflammatory reactions in the airways has been documented in epidemiological studies in children [11, 12], indicating more subtle but long-lasting effects of styrene indoor exposure. Since epidemiological studies provided evidence for such low-dose effects, *in vitro* exposure models for the detailed analysis of VOCs effects on the molecular level were developed [13, 14], allowing the direct exposure of lung epithelial cells with VOCs via the gas phase. Results from *in vitro* studies point to pro-inflammatory effects of styrene and other aromatic VOCs mediated by the production of altered patterns of immune-modulating cytokines. After exposure of lung epithelial cells to 100 $\mu g/m^3$ of styrene, chlorobenzene or m-xylene, an increased level of the monocyte chemoattractant protein-1 was detected [14]. This chemokine is known to induce T-cell differentiation toward a Th2 phenotype, with the consequence of an increased susceptibility to allergic hyperreactivity. The production of cytokines can be regarded as an aggregated parameter that reliably detects changes within the cells, but the molecular mechanism how exposure alters cytokine secretion remains elusive.

To unravel the mode of action of sub-toxic styrene concentrations, a proteomic approach using 2-DE was chosen. A similar strategy had been successfully used to elucidate molecular pathways in response to exposure of liver cells to toxic concentrations of N-nitrosomorpholine [15]. The resolution of modern 2-DE allows detection of up to 1,000-3,000 spots per gel, representing as many protein species. By their specific electrophoretic mobility and p*I* they reveal information about posttranslational modifications, besides the mere identity of the protein itself [16], which can be missed by peptide-based shotgun approaches (for a review of liquid chromatography-based quantitative proteomics see [17]). Differentially expressed protein species should yield clues on the mode of action by which styrene affects lung epithelial cells.

The inhalation path of exposure is common to all airborne environmental pollutants. Since the human lung epithelial cell line A549 is the most common model to test pollutant effects,

a 2-DE reference map was created that will be deposited in a public database in order to support future studies.

So the aim of this study was first to create a reference map of A549 cells, then to detect changes on the proteome level caused by incubation with indoor-relevant concentrations of styrene, and finally to establish a model of the molecular response mechanisms to styrene.

2 Material and Methods

2.1. Analysis of styrene

Styrene concentrations were measured by automated headspace gas chromatography with a Varian 3800 gas chromatograph (Varian, Palo Alto, USA) equipped with a CP SIL 5 CB capillary column (film thickness, 0.12 μm; ID, 0.25 mm; length, 25 m) and a flame ionization detector. The chromatographic conditions were as follows: injector temperature, 250°C, split 1:50; detector temperature, 260°C and an oven temperature program consisting of 70°C for 2 min, followed by an increase at a rate of 10°C min^{-1} up to 90°C and then followed by a further increase at a rate of 60°C min^{-1} until 220°C was reached. Helium (1 ml min^{-1}) was used as a carrier gas. Cell culture medium following styrene exposure (diluted 1:10 in 1.6 mM H_2SO_4; final volume, 10 ml) was prepared in 20 ml glass vials. The samples were incubated for 30 min at 70°C in an agitator (rotation regime, 250 rpm for 5 s and no rotation for 2 s) prior to analysis, and 1 ml of each sample's headspace was injected. For calibration, diluted standards (45 μg/l – 4.5 mg/l) of styrene prepared from stock solutions were treated in the same way as the samples. The stock solutions were prepared in pure methanol.

2.2. Cell culture and styrene exposure

Human lung epithelial cells (A549, ATCC No. CCL-185; LGC Promochem, Wesel, Germany) were cultured in RPMI 1640 Medium (5% heat-inactivated FCS, both Biochrom, Berlin, Germany) at 37°C and 5% CO_2. Passages 3-20 were used for exposure experiments. In the last passage prior to the exposure experiment, the cells were adapted to RPMI 1640 medium supplemented with 2.5% FCS, 1% Penicillin/Streptomycin. About $2*10^5$ cells were seeded in cell culture inserts (Anopore membrane, 2.3 cm diameter, pore size 0.2 μm, transparent; Nunc, Langenselbold, Germany) and cultured to about 70% confluence (for 3 days at 37 °C). Upper and lower medium phase were discarded and the inserts were transferred to petri dishes (35×10 mm) containing fresh exposure medium, a mixture of one part CO_2-independent cell culture medium (Gibco Invitrogen Corp., Paisley, UK; including 2 mM N-acetyl-L-alanyl-L-glutamine and 1% BME amino acid cocktail; both Biochrom, Berlin, Germany) and one part RPMI 1640, supplemented with 1% Penicillin/Streptomycin. 3 petri dishes (containing transwell inserts) were placed in each of the pre-warmed wide-necked glass flasks (600 ml volume; Duran Group, Wertheim, Germany). Cells were exposed to styrene (freshly dissolved in methanol; both reagents from Merck (Darmstadt, Germany)) directly via the gas phase by adding 10 μl of the respective dilution and incubating in tightly closed pre-warmed glass flasks, using styrene concentrations of 0.1 mg/m^3 - 10g/m^3 for 24 h at 37°C as described earlier [10, 13].

2.3. Cytotoxicity measurements

Before and after exposure, cell viability and cell numbers were recorded by Trypan blue exclusion following trypsinization of cultured cells. Membrane integrity was additionally measured using the Cytotoxicity Detection Kit (Roche Applied Science, Mannheim, Germany. Leakage of lactate dehydrogenase (LDH) from exposed cells was estimated in culture medium of exposed cells according to the recommendations of the supplier. As a positive control (in duplicate), all cells from one transwell insert were lysed by adding 100

μl of the provided lysis buffer, resulting in maximum free LDH in the culture medium. For all samples (in triplicates), 100 μl cell culture supernatant were centrifuged, incubated with 100 μl reaction mixture for 30 min in the dark at room temperature. The optical density at 500 nm was measured in triplicates using a 96- well plate reader. LDH release was expressed as percent of total cell LDH.

2.4. Protein extraction

Following exposure (see details above), cells of each transwell insert were washed once with PBS and harvested using trypsin for 3 min at 37°C. Cell suspensions of the three transwell inserts exposed in one glass bottle (see details above) were pooled, centrifuged at 2,000 x g for 3 min and the pellets were washed thoroughly 3 times in ice cold PBS. Afterwards, cell pellets were lysed in 300 μl of 20 mM HEPES pH 7.2 including 10% glycerol, 1% Triton X 100, 1 mM EDTA, 0.5% proteinase inhibitor cocktail (Sigma-Aldrich, München, Germany) and 1.25% Benzonase (Merck, Darmstadt, Germany) on ice for 30 min, sonicated 3 times for 30 sec (duty cycle 40%, output control 3) and centrifuged 15 min at 13,000 x g. Protein concentration (about 1-2 mg/ml) of the cytosolic fraction was determined using the DC Protein Assay (Bio-Rad, München, Germany) and BSA (Albumin Fraction V, #1120180025, Merck, Germany) dissolved in lysis buffer as a protein standard. The assay was performed in 96-well plates.

2.5. Two dimensional gel electrophoresis

300 μg of each cytosol (prepared from cultures in transwell inserts, see details above) were precipitated with acetone (100% v/v) at −20°C for 15 min, and the precipitates were centrifuged at 20,000 x g for 15 min. The pellets were dried and resuspended in 400 μl of DeStreak rehydration solution containing 0.5% IPG-buffer 3-10 NL (both reagents GE Healthcare, Freiburg, Germany). Samples were centrifuged at 20,000 x g for 30 min at 20°C. The supernatant containing the soluble proteins was applied to the wells of a rehydration tray. The 2-DE was performed as described earlier [18]. In brief, IPG strips (18 cm, pH range 3-10 NL; GE Healthcare, Freiburg, Germany) were rehydrated overnight and focused for 100,000 Vhrs using an Ettan IPGphor 3 isoelectric focusing unit (GE Healthcare, Freiburg, Germany). Strips were equilibrated for 15 min with 20 mg/ml DTE and proteins were subsequently alkylated for 15 min in 25 mg/ml iodoacetamide (both dissolved in equilibration buffer, containing 6 M urea, 30% glycerol, 4% SDS, 0.05 M Tris/HCl, bromophenol blue). Strips were run on 12% SDS-PAGE. Gels were stained with CBB G250 (Merck, Darmstadt, Germany) according to Neuhoff *et al.*[19], scanned and dried between cellophane sheets (Bio-Rad, München, Germany).

2.6. Quantitative gel analysis

Gel pictures were scanned using Image scanner II (Amersham Biosciences, United Kingdom) and analyzed in Delta 2D version 3.6 software (Decodon GmbH, Greifswald, Germany; [20]). After warping the gels using the all-to-one strategy, a fusion gel was created including all gels of the experiment. Detected spots were manually edited and transferred to all gel pictures. Spot volumes (integrated staining intensity) were normalized to the total protein amount on each gel (excluding the biggest spots representing ~ 5% of total intensity from the normalization). Relative volumes of the spots were determined. Mean relative volumes of identical spots on triplicate gels (for styrene concentration of 10 g/m^3: duplicate gels) were calculated and divided by the mean relative volume of the corresponding spots in the controls (4 replicates), yielding the expression ratio. Differentially expressed proteins were identified using the following parameters: expression ratio lower than 0.666 or higher than 1.5 and a p-value of $p<0.05$, as obtained by the software's integrated Student's t-test. Proteins were cut from dried gels and identified by

mass spectrometry if they were significantly up- or down-regulated by styrene in at least one of the five different experimental settings.

2.7. Identification of protein spots

Tryptic digestion was carried out with porcine trypsin as described by Benndorf and co-workers [21]. The extracted peptides were either spotted on a MALDI anchor chip target using HCCA matrix (0.6 mg/ml) and analyzed using a Bruker Ultraflex III according to Georgieva *et al.* [22] or were separated by reversed-phase nano-LC (LC1100 series, Agilent Technologies, Palo Alto, California; column: Zorbax 300SB-C18, 3.5 μm, 150 × 0.075 mm; eluent: 0.1% formic acid, 0-60% ACN) and analyzed by tandem mass spectrometry (LC/MSD TRAP XCT mass spectrometer, Agilent Technologies, Palo Alto, California) as described elsewhere [23]. Database searches were carried out using the MS/MS ion search (MASCOT, http://www.matrixscience.com) against all entries of the Swiss-Prot database (http://www.expasy.org) using the subsequent parameters: trypsin digestion, up to one missed cleavage, fixed modifications: carbamidomethyl (C), and with the following variable modifications: oxidation (M), peptide tol.: ± 1.2 Da, MS/MS tol.: ± 0.6 Da and peptide charge: +1, +2 and +3. Proteins were specified as unambiguously identified if the Mowse score was higher than 100 and at least 2 different peptides ($p<0.05$) were used for identification. Molecular weight and p*I* of the identified protein were cross-checked with the gel position of the excised spot. When a significant difference between experimental and theoretical p*I* and/or molecular weight was noticed, we searched for reported protein isoforms or posttranslational modifications that could explain the observed shift using Swiss-Prot database and NetPhos 2.0 Server (http://www.cbs.dtu.dk/services/NetPhos; [24, 25]) .

2.8. Immunoblot analysis

Exposed cells were lysed as described above. 5 - 20 μg of protein extract were used for SDS-PAGE on 12% gels. 20 μg of cytosolic protein were used for every lane in western blots specific for SOD1 and HSP27, whereas only 5 μg of cytosolic protein were used for every lane in western blots specific for VDAC2. Gels were electro-blotted using tank blotting on Optitran BA-S83 Reinforced Nitrocellulose (Whatman, Dassel, Germany) for 2 h at 100 V and 12°C in CAPS buffer (10 mM CAPS, pH 11, 10% methanol). Protein bands were stained with Ponceau S. Blotting efficiency was controlled by staining the gels with CBB G250. Membranes were incubated for 1h in 5% skimmed milk in TBS including 0.1% Tween 20 (TBS-T), washed three times 10 min in TBS-T and incubated overnight in the respective primary antibody dilution, containing 2% skimmed milk (or BSA for anti-SOD1) in TBS-T. HSP27-specific monoclonal mouse antibody (#2402, Cell Signaling Technology, 1:1,000), VDAC2-specific polyclonal rabbit antibody (IMG-5817A, Imgenex, 1:1,000) and polyclonal rabbit anti-SOD1 (#1926, Epitomics, 1:5,000) were used for overnight incubation of membranes. After successive washing steps in TBS-T, the horseradish peroxidase-conjugated secondary antibody (goat anti-mouse (#A4416, Sigma-Aldrich) or goat anti-rabbit antibody (#170-6515, Bio-Rad Laboratories) was added and incubated for 1.5 h at RT. Chemiluminescence signal was measured using Amersham ECL Advance Western Blotting detection kit (GE Healthcare, Freiburg, Germany) and a FluorChem™ 8900 imager (Alpha Innotech, San Leandro, USA). All measurements were normalized to beta-actin signals using monoclonal anti-β-actin antibody (Sigma-Aldrich, München, Germany, clone AC-74, 1:5,000 in 2% milk) using the same immunoblots after stripping at 70°C for 30 min (62.5 mM Tris, 2% SDS, 100 mM 2-mercaptoethanol, pH 6.7). Immunoblot signals were quantified using the freely available Image J software (http://rsbweb.nih.gov/ij/index.html).

Treatment of cells with the antioxidant N-acetylcysteine (NAC, Sigma-Aldrich, München, Germany) as well as the cell exposure to styrene and cell lysis, SDS-PAGE and western

blotting were carried out as recently published [10]. Cells were cultured on transwell inserts as described in paragraph 2.2 and NAC was added to cell exposure medium at a final concentration of 10 mM for the whole exposure time of 24 h. The protein concentration of cell lysates was estimated and 10 μg of cytosolic protein were used for each gel lane. The detection of human glutathione transferase P1 (monoclonal mouse anti-human GST P1 antibody, #MC-411, Kamiya Biomedical Company, 1:2,000) and human heme oxygenase 1 (polyclonal rabbit anti-human HO-1, #Ab3470, Abcam, 1:2,000) were performed as specified before.

2.9. Measurement of reactive oxygen species

A549 cells (100,000 cells in each well of a 24 well plate) were grown in transwell inserts for 24 h [10]. Cells were washed with PBS and incubated for 30 min with 50 μM of 2′,7′ $DCFH_2$-DA (Sigma-Aldrich, München, Germany ;stock solution in DMSO) at 37°C. Cells were washed again, stimulated with 1 ng/ml rh-TNFα (AL-ImmunoTools, Friesoythe; Germany) and exposed to styrene (10^{-2} g/m^3), methanol (control) or $CdCl_2$ (25 μM, positive control) for 2 h. After a subsequent wash cells were trypsinized for 3 min and resuspended in 250 μl of PBS supplemented with 2.5 % of FCS. Reactive oxygen species were measured in triplicates using BD FACS Calibur™ at 488/525 nm.

2.10. Detection and identification of styrene oxide-protein adducts

For detection of proteins modified by styrene oxide (SO) a recently developed antibody was used [9, 26]. SO protein (BSA) adducts (used as a positive control in western blots and for peptide analysis by MS) were prepared using a procedure published by Yuan *et al.* [9] with slight modifications: BSA (Albumin Fraction V, #1120180025, Merck, Germany) was dissolved in PBS. BSA (final concentration of 55 mg/ml) and SO (final concentration of 7.5 mM diluted in DMSO, #77950, Sigma-Aldrich, Germany) were mixed at a ratio of 4:1 (v/v) in a total volume of 2 ml. The solution was incubated overnight under continuous shaking and dialyzed using a Slide-A-lyzer Dialysis Cassette (10,000 MWCO, Pierce Biotechnology, Rockford, Illinois, United States) three times against one liter of aqua dest. for 45 min. Untreated BSA was used as a negative control.

A549 cells were exposed to 100 g/m^3 of styrene for 24 h and together with control cells they were lysed (as described above). 50 μl of the exposed cell culture medium were acetone precipitated. The lysates (200 μg, in duplicates) were analyzed on SDS-PAGE as well as on 7 cm, 3-10 NL 2-DE western blots (for 7 cm 2-DE details see [18, 21]). Nitrocellulose membranes were stained with Ponceau S, scanned and blocked with 5% milk for 1 h and incubated in rabbit SO adduct-specific antiserum #1043 (1:1,000, provided by Jiang Zheng, University of Washington, Seattle, USA) in 2% milk overnight at 4°C. Membranes were washed three times with TBS-T and were incubated in secondary antibody solution (see above) in 2% milk for 1.5 h. 2-DE chemiluminescence images of control and styrene exposed lysates were analyzed using Delta 2D 3.6 software (Decodon GmbH, Greifswald, Germany). Protein spots that were detected with much higher intensity in styrene-exposed lysates were identified from CBB stained 2-DE gels (run in parallel and) prepared from the same sample as the immunoblots. For spot cutting, the Ponceau S (total protein) staining picture of the membrane, which is very similar to the CBB picture of the corresponding gel, was matched with the (SO adduct-specific) chemiluminescence detection picture of the same membrane using Delta 2D 3.6 software. Protein identification was carried out twice.

Covalent modification of cytosolic proteins was also analyzed by nano-HPLC/nano-ESI MS. 2-DE Spots (ID 104) of SO-modified proteins (identified with SO-specific antibody) as well as a band of 5 μg of prepared styrene-oxidized BSA (see preparation of SO adducted BSA above) were cut from CBB stained gels. A band of 5 μg of untreated BSA and 2-DE spots

(ID 104) cut from a control gel served as negative controls. Tryptic digest and identification of the spots were carried out as described above using nano-HPLC/nano-ESI MS. Extracted peptides were reconstituted with 50 μl of 0.1 % formic acid, 3 % ACN. 8 μl of 0.1 % formic acid, 3 % ACN were added to 2 μl of the reconstituted peptides (the remaining volume was stored at −20°C) for further dilution. The peptide solution was added to a 96-well plate. The injection volume was set to 8 μl. Identification of SO modified peptides of thioreductase 1 (isoform 5) were carried out using BioTools 3.0 and Sequence Editor (Bruker Daltonik, Bremen, Germany) using the subsequent parameters: trypsin digestion, up to one missed cleavage, variable modifications: oxidation (M), styrene oxide (Asp, Glu, His, Lys or Secys, Cys), peptide tol.: ± 1.2 Da, MS/MS tol.: ± 0.6 Da and peptide charge: +1, +2 and +3.

3 Results and discussion

3.1. Cell culture model and exposure of cells to styrene

In this study, transwell inserts were used for the most direct exposure of the cells to styrene via the gas phase. The cells were nourished through membrane pores from the basal side while being exposed directly to the gas phase above them [10, 13, 14].

The cells' actual exposure to styrene was calculated by monitoring the distribution of the applied volatile substance between air and medium phase. Styrene concentrations in cell culture medium were analyzed after 24 h of exposure to 0.1 g, 1 g and 10 g styrene/m^3 gas atmosphere (= 23.5 - 2350 ppm). This resulted in styrene concentrations of 0.2 – 20 mg/l (Fig. 1A; 1.93 μM - 191.8 μM*)* in the cell culture medium. No styrene could be detected in media of control cells which were not exposed to styrene. Increased solvent (methanol) volumes resulted in slightly increased styrene concentrations in the medium. Styrene concentrations in the liquid phase did not change significantly when water or PBS was used instead of culture medium (data not shown). The mean partition coefficient (cmedium/cgas 24 h) was calculated to be 2.02 ± 0.02, which corresponds well with published data. Gargas and Andersen determined a partition coefficient ($c0.9\%NaCl/c_{gas}$) of 1.41±0.47 for styrene [27], whereas Sato and Nakajima published a styrene partition coefficient (c_{aqua}/c_{gas}) of 4.68±0.31 [28]. These partition coefficients, together with the relatively small medium phase (2 ml vs. 600 ml gas phase) ensured that applied styrene concentrations remained essentially unchanged during the experiments.

3.2. Toxicity studies

We analyzed cell toxicity of styrene for human lung epithelial cells exposed directly via the gas phase. Total cell number and cell viability were measured by Trypan blue exclusion after 24 h of exposure. The total cell number decreased to 69.6% relative to control cells following exposure to 100 g/m^3 styrene. With decreasing styrene concentration total cell number reached 77.4% (10 g/m^3, 0,19 mM) and 88.1% (1g/m^3, 0.019 mM) relative to control cells (data not shown). Croute *et al.* observed a growth inhibition of 80-90% in studies using A549 cells in exposure experiments over 4 days with 1 mM, one order of magnitude higher than used in our experiments, of ethylbenzene, xylene or monochlorobenzene. At lower concentrations a similar growth inhibition (7-20%) compared to our study was found [29].

Control cells showed a high viability (92%) under the exposure conditions (no serum supplementation, growth on membrane inserts, trypsinization). Viability of exposed cells decreased with increasing concentration of styrene to 40% relative to control cells upon exposure to 100 g/m^3 (Fig. 1B). Diodovich *et al.* demonstrated that after 24 and 48 h of exposure, styrene (0.8 mM) induced an increase in the necrosis of mononuclear cord blood cells [30].

We assessed membrane damage by measuring lactate dehydrogenase (LDH) release into the cell culture medium (Fig. 1C). LDH release within 24 h increased up to 20% of total cellular LDH compared to control cultures (only 5% of LDH total) when cells were exposed to 100 g/m^3 styrene. No membrane damage could be detected when exposing cells to lower concentrations.

From the collected toxicity data we derived a No Observed Effect Concentration (NOEC) of 10 mg/m^3 following a 24 h exposure in this experimental set-up.

3.3. Differential protein expression following styrene exposure

We detected 1,380 protein spots of A549 cells by 2-DE and identified 266 of these spots by tryptic digest and mass spectrometric analysis of the peptides in order to create a proteome map for further projects (Fig. 2A). Here we present the first proteome map of this cell line to this extent. The collected identification data (see supplemental table 1) are in good agreement with published proteome data on A549 cells [31].

In our study we applied five styrene concentrations (1 mg/m^3, 10 mg/m^3,100 mg/m^3, 1 g/m^3 and 10 g/m^3 for differential protein expression analysis in gel replicates (two to four replicates). Using 10 mg (2.3 ppm) and 1 mg styrene/m^3 (0.23 ppm), we applied environmentally relevant concentrations. We quantified the expression of about 1,380 protein spots of A549 cells with p*I* between 3 and 10 using Delta 2D 3.6 software. The reproducibility of the gels was confirmed by unsupervised cluster analysis, by which the comparisons between the different samples and the controls showed a clear clustering according to the experiments (heatmaps are shown in supplemental figures 1 and 2). We identified 64 protein spots displaying a difference in expression stronger than 1.5 fold ($p<0.05$) in at least one of five styrene concentrations between 10 g and 1 mg/m^3 (Fig. 2B, table 1). A total of 21 protein spots were significantly changed in at least two, 11 protein spots in at least three of five styrene exposure concentrations. The highest number of protein expression changes was observed in the two highest styrene concentrations applied. Following exposure to 10 g/m^3, 17 proteins were up- and 6 were down-regulated. When applying 1 g/m^3, 27 proteins were significantly up- and 8 were down-regulated. Using lower concentrations we observed less differentially expressed proteins (100 mg/m^3: 5 up, 7 down; 10 mg/m^3: 7 up, 5 down; 1 mg/m^3: 12 up, 4 down). A set of 16 protein spots was found to be significantly altered due to exposure to styrene at environmentally significant concentrations of 1-10 mg/m^3 (0.2 – 2.3 ppm). In general, we detected more induced than repressed protein spots. Significantly regulated protein species are listed in table 1 and a subset is displayed in more detail in figure 2. Some proteins changed their expression in a roughly concentration-dependent manner, e.g. transaldolase, moesin, thioredoxin reductase 1 or protein DJ-1. However, for most regulated protein spots we did not observe a direct correlation between expression modulation and exposure concentration.

Identified proteins with modulated expression after exposure to styrene are involved in different cellular processes such as oxidative stress regulation (16) inflammation (4), cell death signaling (14), protein quality control (8) and metabolism (11).

3.4. Styrene exposure modulates oxidative stress proteins

Intriguingly, we identified several redox-sensitive proteins susceptible to styrene exposure. Superoxide dismutase [Cu-Zn] expression was increased by a factor of 1.51 at a concentration of 1 mg/m^3 ($p<0.01$) and by a factor of 1.72 ($p<0.03$) when cells were exposed to 100 mg/m^3.

Human biliverdin reductase A (BLVRA) exerts 3% of its total activity in lung cells. Increased expression of BLVRA (1.6 and 1.89, $p<0.01$), catalyzing the reaction of biliverdin

to bilirubin, a potent cytoprotectant, was observed following exposure to 10 g/m^3 and 1 mg/m^3. In the presence of biliverdin, which is supplied by heme oxygenase-1, an inducible stress protein [32, 33], BLVRA is able to form a redox cycle that eliminates pro-oxidant species with concomitant consumption of NADPH [34]. Ahmad *et al.* identified BLVRA as a leucine zipper-like DNA-binding protein that functions in transcriptional activation of heme oxygenase-1 by oxidative stress events [35]. Baranano *et al.* reported the depletion of cellular bilirubin by RNA interference of BLVRA and by this way augmented tissue levels of reactive oxygen species, resulting in cell death [34]. The increased level of BLVRA in our experiments can be interpreted as a response mechanism to overcome styrene-induced oxidative stress.

DJ-1 protein is a known indicator of oxidative stress [36] that may function as a redox-sensitive molecular chaperone, protecting cells against the effects of oxidative stress [37]. The protein was induced significantly at 3 of 5 styrene concentrations.

Clic1**,** a redox sensitive ion channel and a member of the GST family [38] was up-regulated by up to 250% when exposed to 1g/m^3 of styrene.

In addition, we identified several enzymes of the pentose phosphate pathway (PPP) to be differentially expressed. Synthesis of reduced glutathione from the oxidized form is completely dependent on NADPH produced by this pathway [39], [40]. Transaldolase 1 (TALDO1) showed a more than doubled expression at styrene concentrations of 10 g/m^3 and 1 g/m^3. The expression was increased to a lesser extent at lower exposure concentrations. TALDO1 acts as key enzyme of the non-oxidative branch of the PPP. Banki *et al.* proposed that GSH levels and sensitivity to apoptosis are regulated by changes in TALDO1 expression in human cells [39].

6-phosphogluconate dehydrogenase (PGD), which is also involved in NADPH synthesis, was significantly up-regulated by more than a factor of 2 when exposed to 1 g/m^3 styrene. In cells exposed to 10 g/m^3 or 10 mg/m^3 of styrene, the spot was detected with increased intensity compared to control cells but with lower significance ($p<0.1$). Kozar *et al.* observed stimulation of the PPP including PGD during the recovery period from acute lung injury and concluded that both the PPP and the GSH system contribute to the recovery phase of oxidant-mediated lung injury [41].

We found expression of aldehyde reductase (AR) to be doubled when exposed to 1 g/m^3 styrene. AR catalyzes the NADPH-dependent reduction of a wide variety of carbonyl-containing compounds to the corresponding alcohols, with a broad range of catalytic efficiencies [42]. Aldehyde dehydrogenase 3A1, which is also involved in the metabolism of xenobiotics [43], showed increased expression at 3 of 5 exposure levels.

In conclusion, the early molecular response of the cells in this model seems to be governed by an oxidative stress response, which is in concordance with epidemiological data that could associate VOC burden with biomarkers of oxidative stress in the urine of patients [44].

3.5. Styrene exposure may stimulate an inflammatory process via NF-kappa B activation

The observed doubling in expression of annexin A7 at concentrations of 10 and 1 g/m^3 as well as 1 mg/m^3 may be indicative for stimulated secretion of lung surfactant since annexin A7 promotes membrane fusion during exocytosis in alveolar type II cells [45, 46]. Increased lung surfactant protein secretion delimitates lung injury during non-infectious and inflammatory challenge [47].

Heat shock protein B1 (HSPB1) expression was decreased to a level of about 40% (relative to the control) at 10 g/m^3 as well as at 100 mg/m^3 styrene. It has been previously shown that HSPB1 down-regulation results in induction of NF-kappa B (NF-κB) reporter activity and increases the release of the pro-inflammatory cytokine IL-8 in human keratinocytes [48]. Additionally, HSPB1 siRNA increases basal and tumor necrosis factor alpha-mediated activation of the NF-κB pathway in HeLa cells [49].

A two-fold increased expression of moesin, an important molecule for leucocyte adhesion during inflammation, was observed following exposure to styrene. Recent studies have shown that moesin regulates the preservation of alveolar structure and lung homeostasis [50].

Peroxiredoxin 4 expression was limited to 58% relative to the control level when cells were exposed to styrene at a concentration of 100 mg/m^3. Jin *et al.* proposed that in human cells, peroxiredoxin 4 defines a redox-sensitive pathway that specifically regulates NF-κB activity by modulating IκB-α phosphorylation in the cytoplasm. Interestingly, overexpression of peroxiredoxin 4 in HeLa cells resulted in suppression of TNF-dependent NF-κB activation [51]. From this finding we conclude that decreased abundance (or activity) of peroxiredoxin 4 may indicate NF-κB activation.

Evidence for a connection of exposure to VOCs and the NF-κB pathway was also confirmed by a study in which the induction of the NF-κB and the p38 MAP kinase pathway, via a redox-specific mechanism, was shown after exposure to chlorobenzene [52] or styrene [10]

3.6. Styrene affects abundance of apoptosis-related proteins

Nucleoside diphosphate kinase A (NM23-H1), which has recently been identified as a granzyme A (GzmA) -activated, apoptosis-inducing DNase which forms a part of the SET complex [53, 54], showed increased expression at all styrene concentrations, reaching levels of up to 185% relative to control cells at a concentration of 10 g/m^3 ($p<0.01$). In a study by Fan *et al.*, cells with silenced NM23-H1 expression displayed resistance to GzmA-mediated DNA damage and cytolysis, while cells overexpressing NM23-H1 were more sensitive [54].

Annexin A1 is known for its anti-inflammatory function, its involvement in the ERK repression pathway and apoptosis [55]. We found increased expression of annexin A1 at several concentrations, with a more than doubled expression when cells were exposed to 1 g/m^3 of styrene. Annexin A1 was even proposed as a stress protein in A549 cells by Rhee *et al.* [56].

The programmed cell death 6-interacting protein, also known as ALG-2/AIP-complex, is supposed to have a modulating role at the interface between cell proliferation and cell death [57]. The protein was also up-regulated when cells were exposed to 10 g/m^3 styrene.

In contrast, voltage dependent anion channel 2 (VDAC2) showed significantly decreased expression when exposed to styrene at three concentrations (10 mg/m^3, 100 mg/m^3, 10 g/m^3). This mitochondrial outer-membrane protein interacts specifically with the inactive conformer of the multi-domain pro-apoptotic molecule BAK. Reduced levels of VDAC2 make cells more susceptible to apoptotic death [58]. Furthermore, several different lamins, known to undergo proteolysis during apoptosis, revealed reduced expression in the presence of styrene.

Translation initiation factor eIF-5A, a nucleocytoplasmic shuttle protein also playing a role in apoptosis [59], was significantly up-regulated at three styrene concentrations, including the relatively lowest one of 1 mg/m^3.

Two protein spots identified as 60S ribosomal protein L5 (RPL5) were up-regulated in their expression at all concentration levels, with great significance when exposed to 1 g/m^3 or 10 mg/m^3. RPL5 was recently identified as a substrate of death-associated protein kinase (DAPk), a serine/ threonine kinase whose contribution to cell death is well established [60]. In summary, these data provide evidence that styrene, besides oxidative stress, also induces apoptotic pathways to a certain but lower extent.

3.7. Styrene, metabolic changes and protein quality control

A relatively high number (8) of proteins that can be connected to protein quality control, e.g. annexin A1, t-complex protein 1, tumor rejection antigen, heat shock 70kDa protein 4, proteasomal and ribosomal proteins were differentially expressed following styrene exposure as well as proteins involved in the cellular metabolism, e.g. glycyl-tRNA synthetase and glycogen phosphorylase. Several authors emphasized the interrelation of oxidative stress with metabolic changes, although it remains challenging to explain this phenomenon [61, 62].

3.8. Validation of 2-DE results

From each of the three biological pathways, oxidative stress, apoptosis and inflammation, we have initially chosen one protein to validate 2-DE quantification results by an independent method: superoxide dismutase 1 (SOD1), voltage dependent anion channel 2 (VDAC2) and heat shock protein beta 1 (HSPB1), respectively. Using SDS-PAGE and immunoblot for detection of all three proteins from samples obtained after exposure to styrene at concentrations of 1 g/m^3 and 100 $\mu g/m^3$, we were able to confirm the results from 2-DE (Fig. 4A). We observed a slight (10-20%) change in expression at the concentration of 1 g/m^3 for all three proteins. In the cells exposed to the lower concentration of styrene (100 $\mu g/m^3$), we detected a significant ($p<0.05$) increase in expression of SOD1 (174% of control) and a decrease in expression of VDAC2 (47% of control) and HSPB1 (57% of control), similar to what we found in our 2-DE analysis (see table 1).

In addition, we analyzed the protein expression of two typical oxidative stress markers, heme-oxygenase 1 and glutathione transferase P1 in lysates obtained from styrene-treated cells (10^{-4} -10^{-2} g/m^3, Fig. 4B). Both markers showed a more then 2-fold increased expression when compared to controls. Simultaneous treatment of cells with the antioxidant N-acetylcysteine (NAC, 10 mM) inhibited increased expression of stress proteins caused by styrene exposure.

To further strengthen our hypothesis of increased cellular formation of reactive oxygen species (ROS) by exposure to styrene, we measured their internal concentration using 2′,7′-dichlorodihydrofluorescein diacetate. Upon styrene exposure, an increase in the formation of ROS was clearly evident (Fig. 4C). The effect was even stronger than that of a control exposure of A549 to 25 μM of $CdCl_2$.

3.9. Treatment with styrene caused formation of styrene oxide-protein adducts in the cells

It is known that styrene is metabolized to styrene oxide (SO) by cytochrome P450 monoxygenases in exposed cells. Cellular proteins (as well as DNA) react with epoxide metabolites and form protein adducts on cysteine residues. Well-known examples are haemoglobin and serum albumin [7, 8], but here we focused on the analysis of the cytoplasmatic proteins. As a positive control, SO-modified BSA was prepared according to the protocol of Yuan *et al.* [9] with minor modifications. Antibody #1043 (provided by Jiang Zheng; see also [9, 26]) was used in western blotting, yielding a very strong signal in the lane of the positive control (Fig. 5A/B, lane 2), whereas we observed only a low background signal in the negative control lane (BSA, Fig. 5A/B, lane 3) as well as in the lane of the

culture medium control (Fig. 5A/B, lane 1). Additionally, the mass spectrometric analysis of peptides from SO-modified BSA confirmed covalent modifications (Fig. 6A-C, Supplemental figure 3). SO adducts were mainly detected on Cys but also on Asp, Glu, His or Lys as has been reported in earlier studies [63].

Using lysates from styrene-exposed (100 g/m^3) and non-exposed A549 cells for SO-specific standard (Fig. 5A/B, lane 5 and 4, respectively) and 2-DE western blots (Fig. 5 C/D), we were able to detect several significantly altered spots, even in the presence of an unexpectedly high number of non-specifically staining proteins in the control. In the 2-DE western blot, two protein spots were detected at 40 kDa. The bigger one of the two spots was identified as poly (rC)-binding protein 1 whereas the smaller spot remains unidentified so far.

At 55-60 kDa, two spots that seem to be isoforms were detected clearly in lysates of the exposed cells (Fig. 5 D) but barely in control lysates (Fig. 5C). Both protein spots were identified as human thioredoxin reductase 1 [64]. This protein is pivotal for the reduction of thioredoxin, a key element in the control of the cellular redox state [65]. Moreover, recent results linked the functionality of thioredoxin in alveolar epithelial cells directly with the NF-κB pathway [66].

Human thioredoxin reductase 1 contains two redox-active sites. The C-terminal redox center containing selenocysteine (Secys) [cysteine Cys-497, Secys-498] is suggested to carry reducing equivalents from the conserved active sites [Cys-59, Cys-64] to the substrate [67]. The importance of these residues is underlined by the irreversible inhibition after alkylation of both, Cys-497 and Secys-498 [68]. The essential role of the Secys in thioredoxin reductase 1 was demonstrated by further alkylation studies. With alkylation efficiency of >90% in Secys-498, enzyme activity was inhibited nearly completely (99%). Additional modification of the Cys-59, Cys-64 disulfide center [69] was provoked under more severe alkylation conditions.

In this study, we have been able to prove alkylation by SO of thioredoxin reductase 1 by antibody staining. Furthermore we have direct evidence for the alkylation of Secys-498 by the mass spectrometric detection of aa 638-649 (SGASILQAGCUG and aa 637-649 (RSGASILQAGCUG) (Fig. 6 D-E).

4 Concluding remarks

In this study a reference proteome map of a lung epithelial cell line (A549) is provided that will foster future work with these widely used cells. The greatest changes in expression following exposure to styrene at sub-toxic concentrations concerning amplitude and number were found for proteins involved in the oxidative stress response. Further alterations also hint at inflammatory and apoptotic pathways. Naturally the results of this study do not allow delineation of the exact chain of events following styrene exposure, but together with evidence from the literature and considering the specific molecular modification of the thioredoxin reductase 1, an oxidative stress response is the most likely candidate for the initial molecular response mechanism at sub-toxic, but immunologically effective, concentrations of styrene.

Supplementary Material

Refer to Web version on PubMed Central for supplementary material.

Acknowledgments

The authors thank Tobias Friedrich, Yorke Reynolds, Kaley Morris, Yvonne Kullnick, Katrin Schlenz, Franziska Kohse, Michaela Risch and Kerstin Krist for cooperation and technical assistance. Partial support was provided by NIH Grant RO1 HL080226.

Abbreviations

SO	styrene oxide
VOC	volatile organic compound

5 References

[1]. Hodgson M, Levin H, Wolkoff P. Volatile organic compounds and indoor air. J Allergy Clin Immunol. 1994; 94:296–303. [PubMed: 8077582]

[2]. Molhave L. Indoor climate, air pollution, and human comfort. J Expo Anal Environ Epidemiol. 1991; 1:63–81. [PubMed: 1824312]

[3]. Cooke TF. Indoor air pollutants. A literature review. Rev Environ Health. 1991; 9:137–160. [PubMed: 1792387]

[4]. ECIC, European Chemical Industry Council. EC Criteria Document. Brussels: 1994.

[5]. Samet JM, Marbury MC, Spengler JD. Respiratory effects of indoor air pollution. J Allergy Clin Immunol. 1987; 79:685–700. [PubMed: 3571762]

[6]. Tang W, Hemm I, Eisenbrand G. Estimation of human exposure to styrene and ethylbenzene. Toxicology. 2000; 144:39–50. [PubMed: 10781869]

[7]. Yeowell-O'Connell K, Jin Z, Rappaport SM. Determination of albumin and hemoglobin adducts in workers exposed to styrene and styrene oxide. Cancer Epidemiol Biomarkers Prev. 1996; 5:205–215. [PubMed: 8833621]

[8]. Teixeira JP, Gaspar J, Roma-Torres J, Silva S, et al. Styrene-oxide N-terminal valine haemoglobin adducts in reinforced plastic workers: possible influence of genetic polymorphism of drug-metabolising enzymes. Toxicology. 2007; 237:58–64. [PubMed: 17566625]

[9]. Yuan W, Chung J, Gee S, Hammock BD, Zheng J. Development of polyclonal antibodies for the detection of styrene oxide modified proteins. Chem Res Toxicol. 2007; 20:316–321. [PubMed: 17266334]

[10]. Roder-Stolinski C, Fischader G, Oostingh GJ, Feltens R, et al. Styrene induces an inflammatory response in human lung epithelial cells via oxidative stress and NF-kappaB activation. Toxicol Appl Pharmacol. 2008; 231:241–247. [PubMed: 18554678]

[11]. Diez U, Kroessner T, Rehwagen M, Richter M, et al. Effects of indoor painting and smoking on airway symptoms in atopy risk children in the first year of life results of the LARS-study. Leipzig Allergy High-Risk Children Study. Int J Hyg Environ Health. 2000; 203:23–28. [PubMed: 10956586]

[12]. Diez U, Rehwagen M, Rolle-Kampczyk U, Wetzig H, et al. Redecoration of apartments promotes obstructive bronchitis in atopy risk infants--results of the LARS Study. Int J Hyg Environ Health. 2003; 206:173–179. [PubMed: 12872525]

[13]. Lehmann I, Roder-Stolinski C, Nieber K, Fischader G. In vitro models for the assessment of inflammatory and immuno-modulatory effects of the volatile organic compound chlorobenzene. Exp Toxicol Pathol. 2008; 60:185–193. [PubMed: 18514500]

[14]. Fischader G, Roder-Stolinski C, Wichmann G, Nieber K, Lehmann I. Release of MCP-1 and IL-8 from lung epithelial cells exposed to volatile organic compounds. Toxicol In Vitro. 2008; 22:359–366. [PubMed: 17993253]

[15]. Kroger M, Hellmann J, Toldo L, Gluckmann M, et al. [Toxicoproteomics: first experiences in a BMBF-study]. Altex. 2004; 21(Suppl 3):28–40. [PubMed: 15057406]

[16]. Jungblut PR, Holzhutter HG, Apweiler R, Schluter H. The speciation of the proteome. Chem Cent J. 2008; 2:16. [PubMed: 18638390]

[17]. Ong SE, Mann M. Mass spectrometry-based proteomics turns quantitative. Nat Chem Biol. 2005; 1:252–262. [PubMed: 16408053]

[18]. Benndorf D, Muller A, Bock K, Manuwald O, et al. Identification of spore allergens from the indoor mould Aspergillus versicolor. Allergy. 2008; 63:454–460. [PubMed: 18315733]

[19]. Neuhoff V, Arold N, Taube D, Ehrhardt W. Improved staining of proteins in polyacrylamide gels including isoelectric focusing gels with clear background at nanogram sensitivity using Coomassie Brilliant Blue G-250 and R-250. Electrophoresis. 1988; 9:255–262. [PubMed: 2466658]

[20]. Berth M, Moser FM, Kolbe M, Bernhardt J. The state of the art in the analysis of two-dimensional gel electrophoresis images. Appl Microbiol Biotechnol. 2007; 76:1223–1243. [PubMed: 17713763]

[21]. Benndorf D, Balcke GU, Harms H, von Bergen M. Functional metaproteome analysis of protein extracts from contaminated soil and groundwater. Isme J. 2007; 1:224–234. [PubMed: 18043633]

[22]. Georgieva D, Risch M, Kardas A, Buck F, et al. Comparative analysis of the venom proteomes of Vipera ammodytes ammodytes and Vipera ammodytes meridionalis. J Proteome Res. 2008; 7:866–886. [PubMed: 18257516]

[23]. Jehmlich N, Schmidt F, von Bergen M, Richnow HH, Vogt C. Protein-based stable isotope probing (Protein-SIP) reveals active species within anoxic mixed cultures. Isme J. 2008

[24]. Blom N, Gammeltoft S, Brunak S. Sequence and structure-based prediction of eukaryotic protein phosphorylation sites. J Mol Biol. 1999; 294:1351–1362. [PubMed: 10600390]

[25]. Zhu K, Zhao J, Lubman DM, Miller FR, Barder TJ. Protein pI shifts due to posttranslational modifications in the separation and characterization of proteins. Anal Chem. 2005; 77:2745–2755. [PubMed: 15859589]

[26]. Chung JK, Yuan W, Liu G, Zheng J. Investigation of bioactivation and toxicity of styrene in CYP2E1 transgenic cells. Toxicology. 2006; 226:99–106. [PubMed: 16872732]

[27]. Gargas ML, Andersen ME. Determining kinetic constants of chlorinated ethane metabolism in the rat from rates of exhalation. Toxicol Appl Pharmacol. 1989; 99:344–353. [PubMed: 2734795]

[28]. Sato A, Nakajima T. Partition coefficients of some aromatic hydrocarbons and ketones in water, blood and oil. Br J Ind Med. 1979; 36:231–234. [PubMed: 500783]

[29]. Croute F, Poinsot J, Gaubin Y, Beau B, et al. Volatile organic compounds cytotoxicity and expression of HSP72, HSP90 and GRP78 stress proteins in cultured human cells. Biochim Biophys Acta. 2002; 1591:147–155. [PubMed: 12183065]

[30]. Diodovich C, Bianchi MG, Bowe G, Acquati F, et al. Response of human cord blood cells to styrene exposure: evaluation of its effects on apoptosis and gene expression by genomic technology. Toxicology. 2004; 200:145–157. [PubMed: 15212811]

[31]. Myung JK, Afjehi-Sadat L, Felizardo-Cabatic M, Slavc I, Lubec G. Expressional patterns of chaperones in ten human tumor cell lines. Proteome Sci. 2004; 2:8. [PubMed: 15598346]

[32]. Slebos DJ, Ryter SW, Choi AM. Heme oxygenase-1 and carbon monoxide in pulmonary medicine. Respir Res. 2003; 4:7. [PubMed: 12964953]

[33]. Slebos DJ, Ryter SW, van der Toorn M, Liu F, et al. Mitochondrial localization and function of heme oxygenase-1 in cigarette smoke-induced cell death. Am J Respir Cell Mol Biol. 2007; 36:409–417. [PubMed: 17079780]

[34]. Baranano DE, Rao M, Ferris CD, Snyder SH. Biliverdin reductase: a major physiologic cytoprotectant. Proc Natl Acad Sci U S A. 2002; 99:16093–16098. [PubMed: 12456881]

[35]. Ahmad Z, Salim M, Maines MD. Human biliverdin reductase is a leucine zipper-like DNA-binding protein and functions in transcriptional activation of heme oxygenase-1 by oxidative stress. J Biol Chem. 2002; 277:9226–9232. [PubMed: 11773068]

[36]. Mitsumoto A, Nakagawa Y. DJ-1 is an indicator for endogenous reactive oxygen species elicited by endotoxin. Free Radic Res. 2001; 35:885–893. [PubMed: 11811539]

[37]. Moore DJ, Dawson VL, Dawson TM. Lessons from Drosophila models of DJ-1 deficiency. Sci Aging Knowledge Environ. 2006; 2006:pe2. [PubMed: 16407572]

[38]. Singh H, Ashley RH. Redox regulation of CLIC1 by cysteine residues associated with the putative channel pore. Biophys J. 2006; 90:1628–1638. [PubMed: 16339885]

[39]. Banki K, Hutter E, Colombo E, Gonchoroff NJ, Perl A. Glutathione levels and sensitivity to apoptosis are regulated by changes in transaldolase expression. J Biol Chem. 1996; 271:32994–33001. [PubMed: 8955144]

[40]. Rho HK, Park J, Suh JH, Kim JB. Transcriptional regulation of mouse 6-phosphogluconate dehydrogenase by ADD1/SREBP1c. Biochem Biophys Res Commun. 2005; 332:288–296. [PubMed: 15896329]

[41]. Kozar RA, Weibel CJ, Cipolla J, Klein AJ, et al. Antioxidant enzymes are induced during recovery from acute lung injury. Crit Care Med. 2000; 28:2486–2491. [PubMed: 10921583]

[42]. Martin HJ, Breyer-Pfaff U, Wsol V, Venz S, et al. Purification and characterization of akr1b10 from human liver: role in carbonyl reduction of xenobiotics. Drug Metab Dispos. 2006; 34:464–470. [PubMed: 16381663]

[43]. Estey T, Piatigorsky J, Lassen N, Vasiliou V. ALDH3A1: a corneal crystallin with diverse functions. Exp Eye Res. 2007; 84:3–12. [PubMed: 16797007]

[44]. Lu CY, Ma YC, Lin JM, Li CY, et al. Oxidative stress associated with indoor air pollution and sick building syndrome-related symptoms among office workers in Taiwan. Inhal Toxicol. 2007; 19:57–65. [PubMed: 17127643]

[45]. Chander A, Chen XL, Naidu DG. A role for diacylglycerol in annexin A7-mediated fusion of lung lamellar bodies. Biochim Biophys Acta. 2007; 1771:1308–1318. [PubMed: 17765009]

[46]. Caohuy H, Pollard HB. Activation of annexin 7 by protein kinase C in vitro and in vivo. J Biol Chem. 2001; 276:12813–12821. [PubMed: 11278415]

[47]. Casey J, Kaplan J, Atochina-Vasserman EN, Gow AJ, et al. Alveolar surfactant protein D content modulates bleomycin-induced lung injury. Am J Respir Crit Care Med. 2005; 172:869–877. [PubMed: 15994463]

[48]. Sur R, Lyte PA, Southall MD. Hsp27 regulates pro-inflammatory mediator release in keratinocytes by modulating NF-kappaB signaling. J Invest Dermatol. 2008; 128:1116–1122. [PubMed: 18007587]

[49]. Park KJ, Gaynor RB, Kwak YT. Heat shock protein 27 association with the I kappa B kinase complex regulates tumor necrosis factor alpha-induced NF-kappa B activation. J Biol Chem. 2003; 278:35272–35278. [PubMed: 12829720]

[50]. Hashimoto S, Amaya F, Matsuyama H, Ueno H, et al. Dysregulation of lung injury and repair in moesin-deficient mice treated with intratracheal bleomycin. Am J Physiol Lung Cell Mol Physiol. 2008

[51]. Jin DY, Chae HZ, Rhee SG, Jeang KT. Regulatory role for a novel human thioredoxin peroxidase in NF-kappaB activation. J Biol Chem. 1997; 272:30952–30961. [PubMed: 9388242]

[52]. Roder-Stolinski C, Fischader G, Oostingh GJ, Eder K, et al. Chlorobenzene induces the NF-kappa B and p38 MAP kinase pathways in lung epithelial cells. Inhal Toxicol. 2008; 20:813–820. [PubMed: 18645721]

[53]. Kaul R, Verma SC, Murakami M, Lan K, et al. Epstein-Barr virus protein can upregulate cyclo-oxygenase-2 expression through association with the suppressor of metastasis Nm23-H1. J Virol. 2006; 80:1321–1331. [PubMed: 16415009]

[54]. Fan Z, Beresford PJ, Oh DY, Zhang D, Lieberman J. Tumor suppressor NM23-H1 is a granzyme A-activated DNase during CTL-mediated apoptosis, and the nucleosome assembly protein SET is its inhibitor. Cell. 2003; 112:659–672. [PubMed: 12628186]

[55]. Debret R, El Btaouri H, Duca L, Rahman I, et al. Annexin A1 processing is associated with caspase-dependent apoptosis in BZR cells. FEBS Lett. 2003; 546:195–202. [PubMed: 12832039]

[56]. Rhee HJ, Kim GY, Huh JW, Kim SW, Na DS. Annexin I is a stress protein induced by heat, oxidative stress and a sulfhydryl-reactive agent. Eur J Biochem. 2000; 267:3220–3225. [PubMed: 10824106]

[57]. Krebs J, Klemenz R. The ALG-2/AIP-complex, a modulator at the interface between cell proliferation and cell death? A hypothesis. Biochim Biophys Acta. 2000; 1498:153–161. [PubMed: 11108958]

[58]. Cheng EH, Sheiko TV, Fisher JK, Craigen WJ, Korsmeyer SJ. VDAC2 inhibits BAK activation and mitochondrial apoptosis. Science. 2003; 301:513–517. [PubMed: 12881569]

[59]. Taylor CA, Sun Z, Cliche DO, Ming H, et al. Eukaryotic translation initiation factor 5A induces apoptosis in colon cancer cells and associates with the nucleus in response to tumour necrosis factor alpha signalling. Exp Cell Res. 2007; 313:437–449. [PubMed: 17187778]

[60]. Bialik S, Berissi H, Kimchi A. A high throughput proteomics screen identifies novel substrates of death-associated protein kinase. Mol Cell Proteomics. 2008; 7:1089–1098. [PubMed: 18283219]

[61]. Kondoh H, Lleonart ME, Bernard D, Gil J. Protection from oxidative stress by enhanced glycolysis; a possible mechanism of cellular immortalization. Histol Histopathol. 2007; 22:85–90. [PubMed: 17128414]

[62]. Lelli SM, San Martin de Viale LC, Mazzetti MB. Response of glucose metabolism enzymes in an acute porphyria model. Role of reactive oxygen species. Toxicology. 2005; 216:49–58. [PubMed: 16125296]

[63]. Phillips DH, Farmer PB. Evidence for DNA and protein binding by styrene and styrene oxide. Crit Rev Toxicol. 1994; 24(Suppl):S35–46. [PubMed: 7818770]

[64]. Dammeyer P, Damdimopoulos AE, Nordman T, Jimenez A, et al. Induction of cell membrane protrusions by the N-terminal glutaredoxin domain of a rare splice variant of human thioredoxin reductase 1. J Biol Chem. 2008; 283:2814–2821. [PubMed: 18042542]

[65]. Burke-Gaffney A, Callister ME, Nakamura H. Thioredoxin: friend or foe in human disease? Trends Pharmacol Sci. 2005; 26:398–404. [PubMed: 15990177]

[66]. Callister ME, Pinhu L, Catley MC, Westwell AD, et al. PMX464, a thiol-reactive quinol and putative thioredoxin inhibitor, inhibits NF-kappaB-dependent proinflammatory activation of alveolar epithelial cells. Br J Pharmacol. 2008

[67]. Mustacich D, Powis G. Thioredoxin reductase. Biochem J. 2000; 346(Pt 1):1–8. [PubMed: 10657232]

[68]. Nordberg J, Zhong L, Holmgren A, Arner ES. Mammalian thioredoxin reductase is irreversibly inhibited by dinitrohalobenzenes by alkylation of both the redox active selenocysteine and its neighboring cysteine residue. J Biol Chem. 1998; 273:10835–10842. [PubMed: 9556556]

[69]. Gorlatov SN, Stadtman TC. Human thioredoxin reductase from HeLa cells: selective alkylation of selenocysteine in the protein inhibits enzyme activity and reduction with NADPH influences affinity to heparin. Proc Natl Acad Sci U S A. 1998; 95:8520–8525. [PubMed: 9671710]

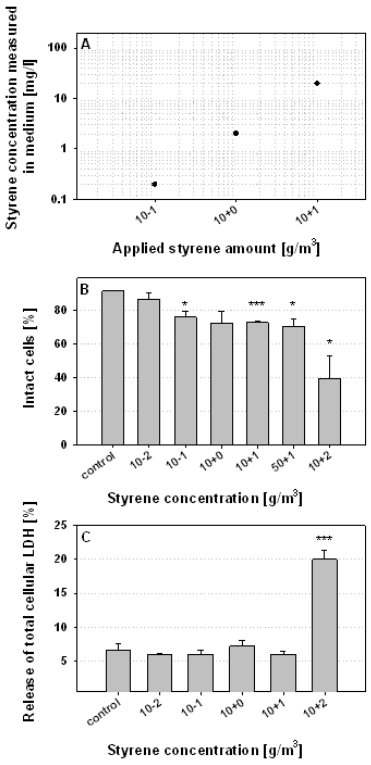

Figure 1.

(A) Styrene medium concentrations following cell exposure with different concentrations of styrene. (B, C) Cell toxicity of styrene exposure was measured using Trypan blue exclusion (B) and lactate dehydrogenase (LDH) release (C). Data are shown as mean of triplicates + SEM. * $p<0.05$, ** $p<0.01$, *** $p<0.001$

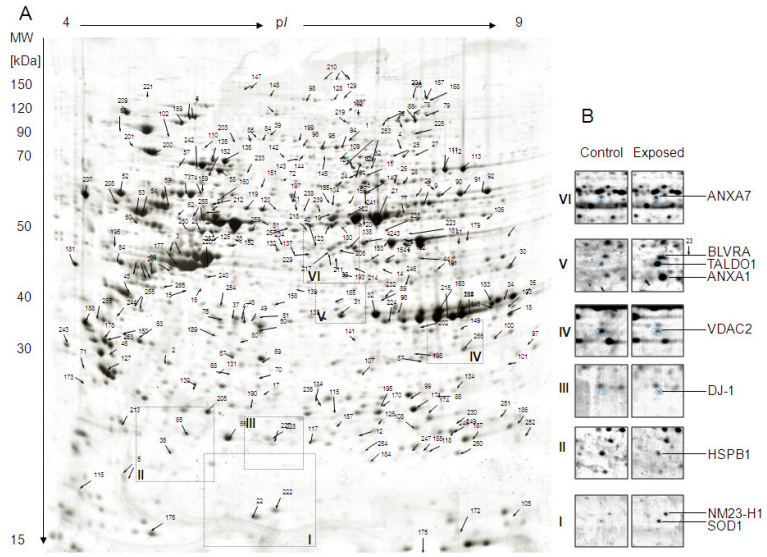

Figure 2.

(A) Proteome map of A549 cell line (identification data are shown in Supplemental table 1). (B) Gel image regions of differentially expressed proteins following styrene exposure. 500 μg of cytosolic protein of A549 cell line were separated by 2-DE (18 cm IPG strips 3-10 NL, 12% acrylamide/bisacrylamide). Abbreviations are gene names.

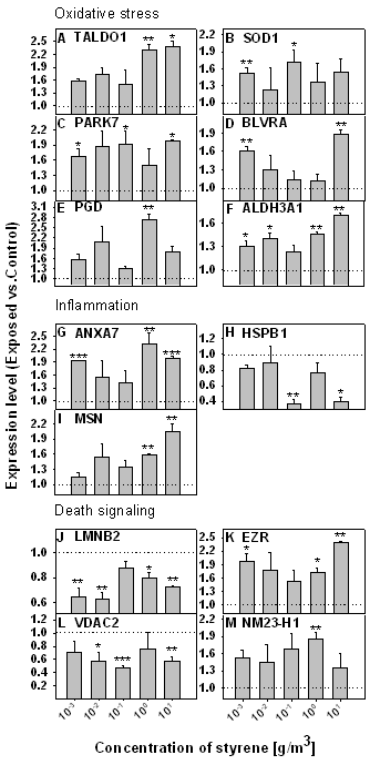

Figure 3.

Cytosolic proteins showing changes in expression after cellular (A549) exposure to styrene. Expression levels are spot volumes relative to spot volumes of control, given as means + SEM of 2-4 replicates. Abbreviations are gene names. * $p<0.05$, ** $p<0.01$, *** $p<0.001$

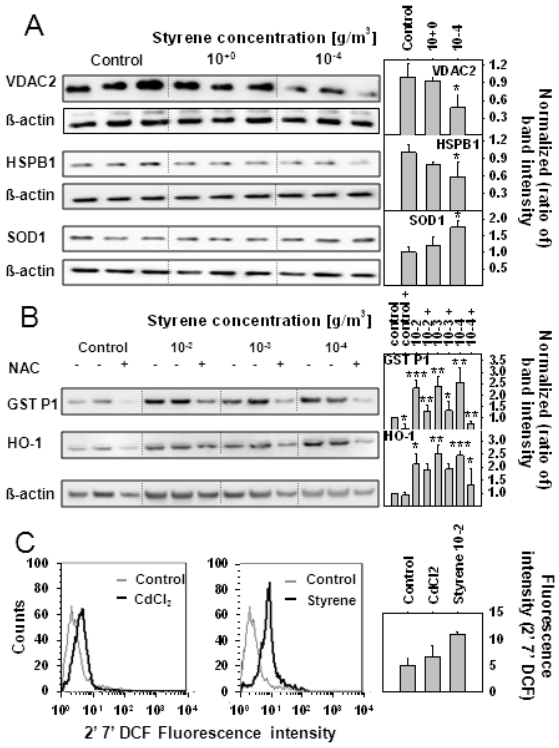

Figure 4.

Validation of 2-DE results. (A) Western blot analysis of A549 cell lysates confirms differential protein expression of superoxide dismutase 1 (SOD1), voltage dependent anion channel 2 (VDAC2) and heat shock protein beta 1 (HSPB1) following cell exposure to styrene. 20 μg of cytosolic protein were used for every lane of western blots against SOD1 and HSPB1, whereas only 5 μg of cytosolic protein were used for every lane of western blot against VDAC2. (B) Treatment of cells with the antioxidant N-acetylcysteine (NAC, 10 mM) inhibited increased expression of stress proteins heme oxygenase 1 (HO-1) and glutathione S transferase 1 (GST P1) caused by styrene exposure. 10 μg of cytosolic protein were loaded for each lane. Beta-actin signals of every lane were used for normalization. Changes in band intensity (arbitrary units) are given relative to the control and calculated as mean of triplicates + SEM. (C) Increased ROS levels in A549 cells following exposure to styrene or cadmium chloride (25 μM). Cells were analyzed for ROS levels by FACS analysis using 2′,7′-dichlorodihydrofluorescein diacetate. ROS levels from one representative experiment as well as the quantification of three independent experiments (mean and standard error of fluorescence intensities) are shown. *p<0.05, ** p<0.01, *** p<0.001.

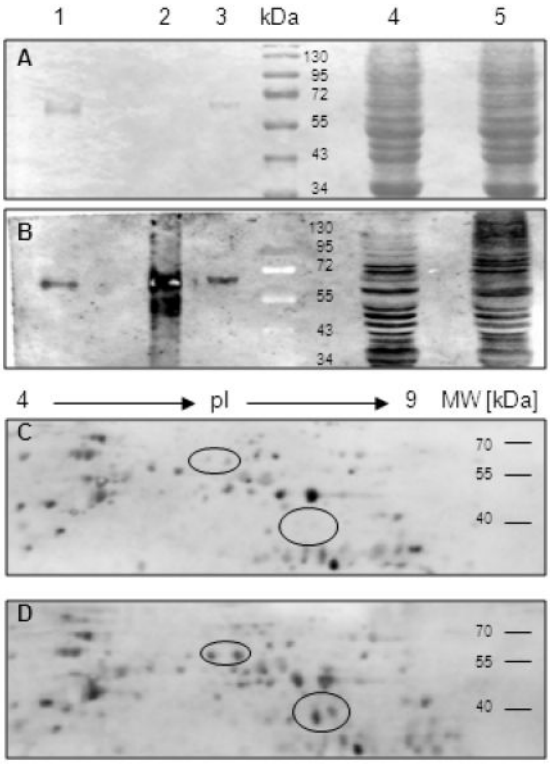

Figure 5.

Standard (A, B) and 2-DE (C, D) western blot analysis of cytosolic styrene oxide (SO)-protein adduct formation following exposure of A549 cells to styrene (100 g/m^3). Figure A (total protein stain Ponceau S) and B (specific detection of protein adducts) prove the sensitivity of the antibody against the positive control (SO-modified BSA, lane 2) in contrast to low detection of untreated BSA (lane 3) and precipitated cell culture medium (lane 1). SO-modified proteins were detected by comparing patterns of lysates (100 μg) of styrene exposed (lane 5) and control (lane 4) cells. The following 2-DE western blot analysis of lysates (200 μg) of control (C) and exposed cells (D) revealed two main areas of differentially detected spot patterns (see circles).

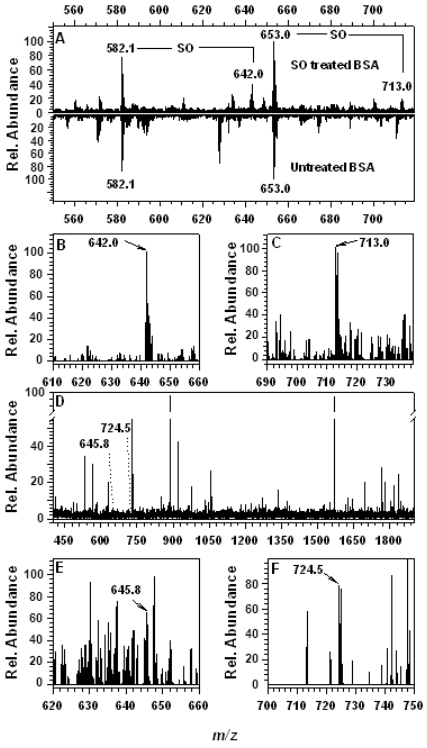

Figure 6.

Nano-HPLC/ESI MS/ (MS) analysis of styrene oxide (SO) adducts of BSA and thioredoxin reductase 1. Sum spectra of SO treated and untreated (control) BSA (A) (m/z 550-720) and human thioredoxin reductase 1 (D) (m/z 400-2000) from styrene treated lung epithelial cells were created with Data Analysis Software. (A) The doubly charged signals of two SO adducts of BSA peptides (aa 66-75, m/z 642.0, Mr_{theo} 1282.7, Δm 0.6, ion score 24 and aa 402-412, m/z 713.0, Mr_{theo} 1424.8, Δm 0.7, ion score 31), which were only detected in the mass spectrum of the treated sample, as well as the corresponding control peptides (m/z 582.1, Mr_{theo} 1162.6, Δm 0.4, ion score 60 and m/z 653.1, Mr_{theo} 1304.7, Δm 0.6, ion score 53), detected in the spectra of the control and the treated sample, are labeled. For modified peptides the mass shift of 120.1 amu (single charged ions), 60.0 amu (doubly charged ions) or 40.0 amu (triply charged ions) induced by the SO adduct formation was detected. (B and C) Enlargements of extracted mass spectra (retention time window 5 min) of the two modified peptides (shown in A). An overview and enlargements of further identified SO adducts are provided in Supplemental figure 3. (E and F) The doubly charged signals (extracted mass spectra, retention time window 1 min) of thioredoxin reductase 1 aa 638-649 (SGASILQAGCUG, C-terminally amidated, m/z 645.8, Mr_{theo} 1289.5, Δm 0.1 Da) and aa 637-649 (RSGASILQAGCUG, m/z 724.5, Mr_{theo} 1446.6, Δm 0.3 Da) are displayed, respectively. Both signals match to a dual alkylation, one Cys or Secys (U) by the reaction with SO (Δm 120.1 amu) and one with iodoacetamide

Table 1

Identified protein spots of differentially expressed proteins following exposure to styrene.

ID [a]	Protein involved in process	Accession [b]	Exposure dependent Expression [c]				
	Oxidative stress		10^{1}	10^{0}	10^{-1}	10^{-2}	10^{-3}
93	Aldehyde reductase	P15121	1.48	2.26 *	1.56	1.40	1.11
123	Aldehyde dehydrogenas e 3A1	P30838	1.70 **	1.46 **	1.23	1.40 *	1.31 *
228	Protein DJ-1	Q99497	1.99 *	1.50	1.91 *	1.86 °	1.67 *
165	Biliverdin reductase A	P53004	1.88 **	1.11	1.14	1.30	1.60 **
184	Peroxiredoxin-1	Q06830	1.71	1.11	1.32	1.20	1.68 °
99	Phosphoglycerate mutase 1	P18669	1.61 °	1.56 °	1.18	1.24	1.25
104	Thioredoxin reductase 1	Q16881	1.57 *	1.38 *	1.13	1.21	1.10
22	Superoxide dismutase [Cu-Zn]	P00441	1.54	1.37	1.72 *	1.24	1.51 **
190	Peroxiredoxin-4	Q13162	0.92	0.72 °	0.58 °	0.75	0.81
110	NADH-ubiquinone oxidoreductase 75 kDa subunit	P28331	1.63 *	0.99	0.89	0.83	1.04
13	Is ocitrate dehydrogenase (NADP)	O75874	1.51 °	1.13	0.92	0.91	0.87
2	Chloride intracellular channel protein 1	O00299	1.01	2.50 ***	1.38 °	0.81	1.00
133	Trans aldolase	P37837	2.37 *	2.29 **	1.50	1.73 °	1.58 °
217	GDI2 protein	Q6IAT1	1.72 *	1.36 °	0.81	1.08	1.10
216	GDI2 protein	Q6IAT1	1.27	1.57 *	1.15	1.18	1.15
161	6-Phosphogluconate dehydrogenase	P52209	1.80 °	2.71 **	1.30	2.07	1.55
	Inflammation						
211	Annexin A7	Q5T0M6	1.98 ***	2.31 **	1.42	1.56	1.92 ***
109	Moesin	P26038	2.05 **	1.59 **	1.34 °	1.54	1.15
36	Heat shock protein beta-1	P04792	0.40 *	0.77	0.37 **	0.90	0.83
224	Annexin A2	Q8TBV2	1.64 *	1.64 °	1.07	1.37	1.15
	Cell death signaling						

Proteomics. Author manuscript; available in PMC 2012 October 03.

ID [a]	Protein involved in process	Accession [b]	Exposure dependent Expression [c]				
94	Ezrin	P15311	2.38 **	1.73 *	1.54	1.77	1.96 *
70	Annexin A4	P09525	2.01	1.00	1.12	1.18	1,86 °
68	Annexin A4	P09525	1.55 *	1.04	1.08	0.76	1.22
57	Laminin subunit beta-1	P07942	0.70	0.38 *	0.78	0.54	0.65
150	60S ribosomal protein L5	P46777	2.11 °	2.06 *	1.85	2.24 *	1.30
244	60S ribosomal protein L5	P46777	3.79	5.02 ***	1.92	4.70 °	1.93
182	Lamin-B2	Q03252	0.72 **	0.79 *	0.87	0.62 **	0.64 **
63	Annexin A5	P08758	1.22 *	0.28	1.76 *	1.35	1.29
213	Tumor protein translationally-controlled 1	Q5W0H4	0.67	0.77	2.82 ***	1.46	0.98
100	Voltage-dependent anion-selective channel protein 1	P21796	0.42 °	0.61	0.91	0.90	0.72
176	Eukaryotic translation initiation factor 5A-1	P63241	1.38	2.77 *	1.16	2.04 *	1.51 **
219	PDCD6IP protein	Q6NUS1	1.87 **	1.32	1.09	1.42	1.13
149	Voltage-dependent anion-selective channel protein 2	P45880	0.58 **	0.61	0.47 ***	0.57 *	0.70
222	Nucleoside diphosphate kinase	P15531	1.34	1.84 **	1.68 °	1.44	1.51 °
	Protein quality control						
31	Annexin A1	P04083	1.65 °	2.11 *	1.43	1.46	1.42
209	Tumor rejection antigen (Gp96) 1	Q5CAQ5	0.61	0.26 *	1.30	0.21 *	0.44 °
203	Eukaryotic translation initiation factor 4B	Q4G0E3	0.19 *	0.26 *	0.26 *	0.63	0.34 °
206	Proteasome 26S non-ATPas e subunit 11	Q53FT5	1.51	1.54 **	1.37	1.03	1.14
160	T-complex protein 1 subunit theta	P50990	0.93	0.33 *	0.84	0.90	0.85
201	Heat shock 70kDa protein 4	Q2TAL4	1.89	1.83	1.06	2.42	5.25 **
243	Ribosomal protein S3a	Q6NXR8	0.58 °	0.36 *	0.69 °	0.44 °	0.76
180	T-complex protein 1 subunit beta	P78371	2.10 °	1.32 °	1.10	1.38 °	1.13
	Metabolism						
106	ATP synthase	P25705	0.74	0.82	0.85	0.56 *	0.74

Proteomics. Author manuscript; available in PMC 2012 October 03.

ID [a]	Protein involved in process	Accession [b]	Exposure dependent Expression [c]				
41	Alpha-enolase	P06733	2.06 *	2.36 *	1.71	1.37	1.77 *
143	Gars protein	P41250	2.34	1.50 *	1.19	1.38	0.94
76	Glycogen phosphorylase	P11216	0.45 **	0.32 **	0.55 *	0.74	0.64 *
39	Gelsolin	P06396	1.77	2.27 *	1.29	1.56	1.18
129	Kinesin-1 heavy chain	P33176	0.87	2.24	0.79	2.39 *	1.50
223	Elongation factor 2b	Q8TA90	2.75 ***	1.37 *	0.64 °	2.44 **	2.03 *
48	L-lactate dehydrogenase	P07195	1.06	0.96	0.50 *	0.60 *	0.83
19	Retinal dehydrogenase 1	P00352	1.76 °	1.33	1.03	1.57 *	1.41 °
126	HNRPH1 protein	P31943	0.61 *	1.60 **	1.01	1.24 *	1.11
125	Cytoc hrome b-c1 complex subunit 1, mitochondrial	P31930	1.02	0.66 °	0.55 *	1.00	0.86

[a] Spot ID from figure 2A

[b] Swiss-Prot Accession

[c] Expression level (exposed vs. control) following exposure to styrene (10-3 to 101 g/m3).

° p<0.1

* p<0.05

** p<0.01

*** p<0.001